International Journal of Information, Control and Computer Sciences
ISSN: 2517-9942
Vol:10, No:2, 2016

Improving Human Hand Localization in Indoor Environment by Using Frequency Domain Analysis

Wipassorn Vinicchayakul, Pichaya Supanakoon, Sathaporn Promwong

***Abstract*—**A human's hand localization is revised by using radar cross section (RCS) measurements with a minimum root mean square (RMS) error matching algorithm on a touchless keypad mock-up model. RCS and frequency transfer function measurements are carried out in an indoor environment on the frequency ranged from 3.0 to 11.0 GHz to cover federal communications commission (FCC) standards. The touchless keypad model is tested in two different distances between the hand and the keypad. The initial distance of 19.50 cm is identical to the heights of transmitting (Tx) and receiving (Rx) antennas, while the second distance is 29.50 cm from the keypad. Moreover, the effects of Rx angles relative to the hand of human factor are considered. The RCS input parameters are compared with power loss parameters at each frequency. From the results, the performance of the RCS input parameters with the second distance, 29.50 cm at 3 GHz is better than the others.

***Keywords*—**Radar cross section (RCS), fingerprint-based localization, minimum root mean square (RMS) error matching algorithm, touchless keypad model.

I. Introduction

NOWADAYS, an indoor localization is applied in many applications such as tracking fire fighter in building of fire, tracking patient in a hospital, tracking miner in mine or finding the item in an industrial [1]-[3].

Many researches try to improve the performance of the indoor localization so the original methods have been considered. The original methods, which are triangulation or lateration (etc.), use received signal strengths (RSS), angles of arrival (AOA), times of arrival (TOA) or time differences of arrival (TDOA) parameters [4], [5] to calculate the location, directly. These methods are not suitable to use in an indoor environment because they are disturbed from the indoor environment. Fingerprinting technique is a technique to solve this problem because it processes the characteristics of a location to record in database and the location process is found from using parameters of the present location to compare with the locations in the database by a pattern matching algorithm [6]-[10].

In this paper, a minimum root mean square (RMS) error matching algorithm is used to find the location because we do not want to worry about error, which obtains from algorithm. Nevertheless, many algorithms are suitable than a minimum RMS error matching algorithm such as Kalman filter, support vector machine and artificial neural network [11].

At the present time, the most localization application uses a transmitter sends the signals to the receiver in order to find the location of receiver or uses the receiver to locate the transmitter. Therefore, we are interested to find out the location of objects without the transmitter or receiver at the object or tag less. The object of interest is a human's hand. Because of in the future, we are going to locate the human location without tag at the human so a touchless keypad mock-up model is created. Furthermore, several research studies have attempted to determine the characteristics of objects (e.g. trees, chairs and a human's body) by using radar cross section (RCS) [12]-[14]. In recent year, there are also advances in the devices for detecting human motion. Most of these devices typically utilize infrared light; however, the detection performance is poor in a strong light environment as the infrared light is disturbed [7]. In this paper human motion detection, the human's hand movement is improved by using RCS measurement. The detection principle for the touchless keypad model is based on the fingerprint-based indoor localization technique.

The purpose of this research is to test the efficiency of frequencies, distances, and parameters for finding the hand location above the keypad. The frequencies are tested in the range 3.0 to 11.0 GHz to cover federal communications commission (FCC) standards [15]. There are two distances, namely 19.50 cm and 29.50 cm. Then, the parameters consist of the power loss parameters and the RCS input parameters.

For the study, the results are shown in terms of the errors of localization. The rest of this paper is organized as follows: Section II is the localization technique. Next the measurement set up is in Section III. After that, experimental results of this paper are explained in Section IV. Finally, the conclusion is given in Section V.

II. The Keypad Processing

A. RCS Input Parameters

In this paper, the RCS input parameters are tested with the keypad. The signal is transmitted in sinusoidal waveform from start frequency to stop frequency by a vector network analyzer (VNA). The RCS input parameters are determined from the radar equation [16]-[18] which describes the relationship between the radar link from transmitter to the target and from the target to receiver in terms of receiving power. Because of the radar equation in the form of the power of the signal, it is first modified in term of voltage of the signal. It can be defined by (1):

Wipassorn Vinicchayakul is a student at the Electrical Engineering Department, Faculty of Engineering, King Mongkut's Institute of Technology Ladkrabang, Bangkok 10520, Thailand (e-mail: s6601033@ kmitl.ac.th).

Pichaya Supanakoon and Sathaporn Promwong are lecturers at the Telecommunication Engineering Department, Faculty of Engineering, King Mongkut's Institute of Technology Ladkrabang, Bangkok 10520, Thailand (e-mail: kspichay@kmitl.ac.th, kpsathap@kmitl.ac.th).

$$V_{\mathrm{r}}(f)=\frac{\lambda e^{-j2\pi f(d_1+d_2)/c}}{(4\pi)^{3/2}d_1d_2}H_{\sigma}(f)H_{\mathrm{t}}(f)H_{\mathrm{r}}(f)V_{\mathrm{t}}(f) \quad (1)$$

where V_r is the received signal, V_t is the transmitted signal, H_t is the transfer function of transmitting (Tx) antenna, H_r is the transfer function of receiving (Rx) antenna, H_σ is the frequency transfer function of scattering, c is the velocity of light, f is a carrier frequency, λ is the wave length, d_1 and d_2 are the distances from the target to Tx and Rx antennas, respectively.

Equation (2) is adjusted to accommodate the ratio of the received signal to transmitted signal in case of obstruction, H_{o}, where H_{o} is obtained by VNA measurements. The adjusted equation can be expressed as

$$H_{\mathrm{o}}(f)=\frac{\lambda e^{-j2\pi f(d_1+d_2)/c}}{(4\pi)^{3/2}d_1d_2}H_{\sigma}(f)H_{\mathrm{t}}(f)H_{\mathrm{r}}(f) \quad (2)$$

Then, the characteristics of Tx and Rx antennas, including H_t and H_r, which are obtained with VNA in an anechoic chamber, are represented in terms of the channel impulse response in free space, H_{f}, which can be written as (3). Parameter d is the distance between Tx and Rx antennas.

$$H_{\mathrm{f}}(f)=\frac{\lambda e^{-j2\pi fd/c}}{4\pi d}H_{\mathrm{t}}(f)H_{\mathrm{r}}(f) \quad (3)$$

Next, to simplify, H_t and H_r are filtered out by dividing (2) by (3). The simplified equation is presented in (4):

$$H_{\sigma}(f)=\frac{H_{\mathrm{o}}(f)}{H_{\mathrm{f}}(f)}\frac{\sqrt{4\pi d_1d_2}}{d}e^{j2\pi f(d_1+d_2-d)/c} \quad (4)$$

After that, the RCS input parameters at different frequencies are determined by analysis of the components of H_σ. Moreover, a RCS input parameter at each frequency, $RI(f)$, can be calculated by (5):

$$RI(f)[dBsm]=10\log(\left|H_{\sigma}(f)\right|^2) \quad (5)$$

B. Power Loss Parameters

The power loss parameters can be obtained from the VNA measurement that defined by (6) [19], where H_{c} is the transfer function of channel measurement.

$$PL_{\mathrm{r}}(f)[dB]=-20\log(\left|H_{\mathrm{c}}(f)\right|) \quad (6)$$

C. Fingerprinting Technique

The fingerprinting technique is a localization technique, which is suitable to manage in the indoor environment. It has two phases: an off-line phase and an on-line phase [7].

In this paper, the off-line phase is a phase to use in order to create the database at each button-cell location by the parameters recording with the button-cell locations. The parameters consist of the parameters from the first Rx antenna, the second Rx antenna and the third Rx antenna. Then, the parameters are the RCS parameters or the power loss parameter. Fig. 1 shows the process of the off-line phase. Then, the on-line phase is used to find the button-cell location by using input parameters at the present location to compare with the parameter in the database with the pattern matching algorithm which is a minimum RMS error matching algorithm. The result of the on-line phase is the hand's location. Fig. 2 shows the process of the on-line phase.

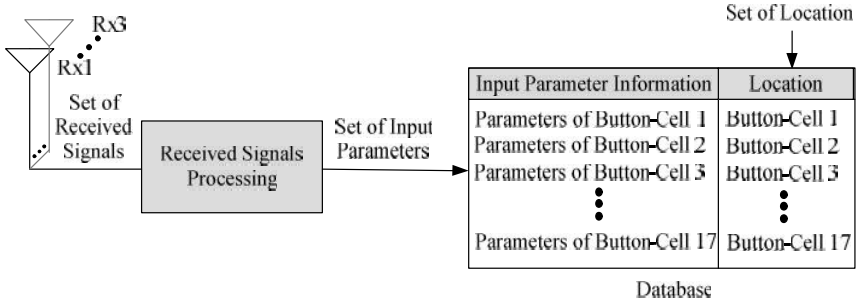

Fig. 1 The fingerprint-based indoor localization technique: off-line phase

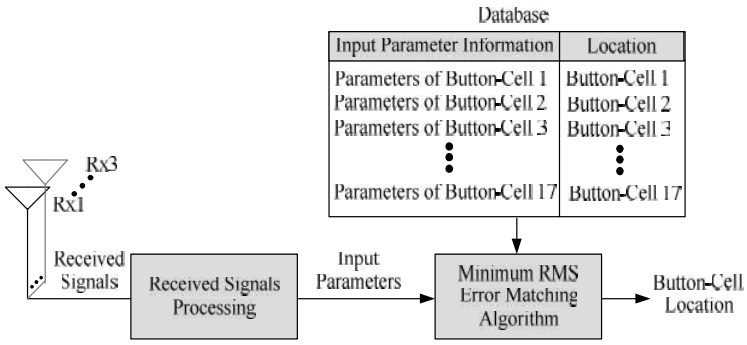

Fig. 2 The fingerprint-based indoor localization technique: on-line phase

D. Minimum RMS Error Matching Algorithm

In this paper, there are two sets of input parameters, namely the RCS input parameters and the power loss parameters for the indoor localization using fingerprint-based technique. The RCS input parameters consist of the RCS input parameters of the first Rx antenna ($RI_1(f)$), the RCS input parameters of the second Rx antenna ($RI_2(f)$) and the RCS input parameters of the third Rx antenna ($RI_3(f)$). The power loss parameters consist of the power loss parameters of the first Rx antenna ($PL_{r1}(f)$), the power loss parameters of the second Rx antenna ($PL_{r2}(f)$) and the power loss parameters of the third Rx antenna ($PL_{r3}(f)$). To obtain minimum RMS errors, the input parameters of the on-line phase are matched against the database of the off-line phase to follow (7):

$$e_k(f,n)=\sqrt{\frac{1}{3}\sum_{i=1}^{3}\left(\frac{[IP_{f(Rx(i))}(f,n)-IP_{t(Rx(i))}(f)]^2}{\sigma^2_{IP_{f(Rx(i))}}}\right)} \quad (7)$$

where IP_f is the parameter in the database, IP_t is the parameter for testing, σ_{IP} is the standard deviations of the input parameter, i is the number of Rx, f is the frequency, n is the reference location. The parameter means the RCS input parameters or the power loss parameters.

The minimum error of all locations is determined by (8).

$$L(f)=\arg\min_{n}\left(e(f,n)\right) \quad (8)$$

where L is the location of a button-cell.

E. Location Accuracy

The performances of the parameters in terms of percentage of location accuracy are determined by (9)

$$\%DA=\frac{N_d}{N_t}\times 100\% \quad (9)$$

where N_d is the number of correct detectable locations and N_t is total number of locations.

III. Measurement Set Up

The experiments were done in an indoor environment in a laboratory of King Mongkut's Institute of Technology Ladkrabang (KMITL)'s Faculty of Engineering. The magnitude and phase of frequency transfer function for each hand location are measured with VNA (HP 8510C). Prior to calibration in full 2-port mode, VNA is set at 3.0 to 11.0 GHz with 801 frequency points. Sweeping time is set at 186 ms and the average function is set at its lowest of 128 to resemble the noise level in real use.

The Tx and Rx antennas are biconical antennas with horizontal polarization [20], [21]. Due to equipment limitation, the heights of Tx and Rx antennas are set at 19.50 cm (the lowest possible) from the tabletop, which is beyond the first Fresnel zone [19]. This paper experiments with the 17 locations, the locations of Rx1-Rx3 relative to the button-cell 3 center are 90°, 180°, and 270°, respectively, while Tx antenna remains stationary at 0°.

We experimented with the touchless keypad model at two different distances between a hand and a paper keypad. The initial distance is 19.50 cm, which is identical to the heights of Tx and Rx antennas. In another setting, the distance between the hand and the keypad is 29.50 cm while the other components remain unchanged. The top view of both settings is illustrated in Fig. 3. Figs. 4 and 5 illustrate the touchless keypad model with the distance between the hand and keypad of 19.50 cm and 29.50 cm, respectively.

IV. Experimental Results

This section attempts to determine the condition or combination that gives the best location accuracy whereby tests are conducted with 3 possible combinations (2x2x17) of three sets of criteria. The three sets of criteria are the parameters (i.e. the RCS parameters and the power loss parameter), distances (19.50 and 29.50 cm) and each frequency (3.0-11.0 GHz, varying 0.5 GHz).

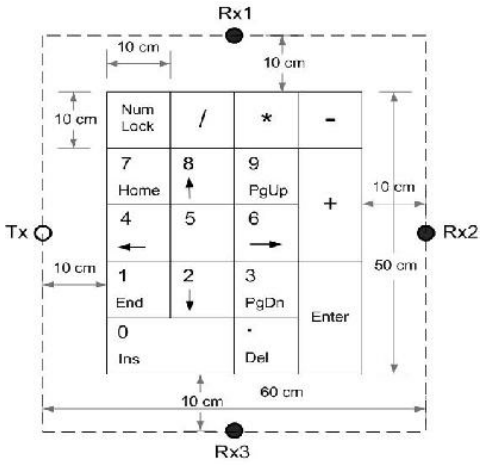

Fig. 3 Top view of the touchless keypad model

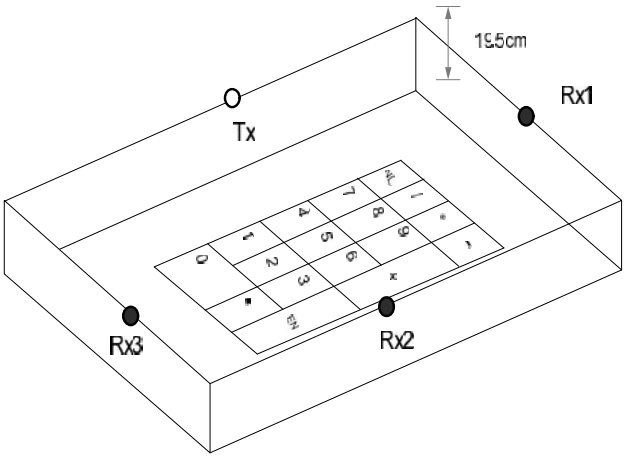

Fig. 4 The touchless keypad model with the distance between the hand and keypad of 19.50 cm

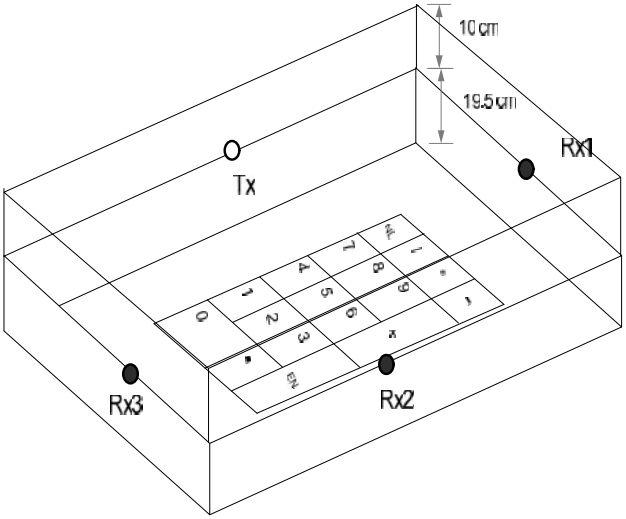

Fig. 5 The touchless keypad model with the distance between the hand and keypad of 29.50 cm

A. Location Accuracy Results

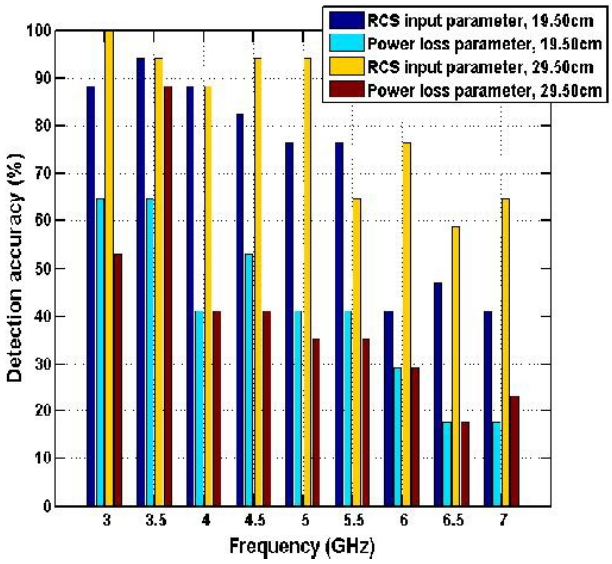

Fig. 6 The accuracy results of touchless keypad model for the frequencies; 3.0-7.0 GHz, varying 0.5 GHz

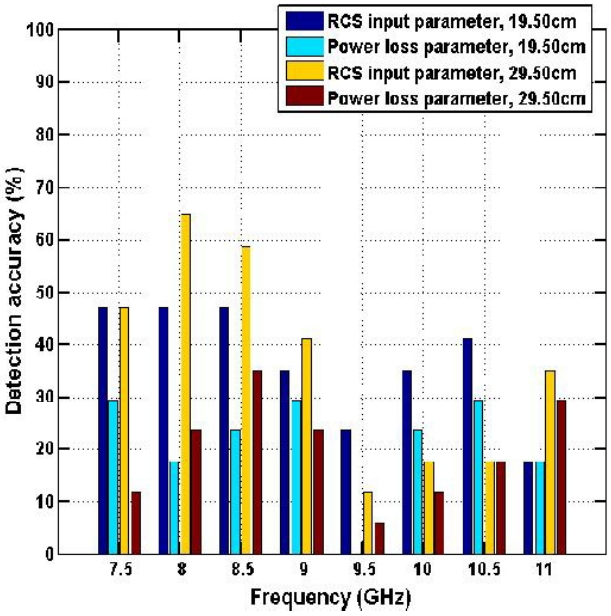

Fig. 7 The accuracy results of touchless keypad model for the frequencies; 7.5-11.0 GHz, varying 0.5 GHz

Figs. 6 and 7 illustrate the keypad model accuracy of the RCS input parameters and the power parameters with the distance of 19.50 cm and 29.50 cm from the frequencies 3.0-11.0 GHz. Then, the RCS input parameters with the distance of 29.50 cm at the frequency 3.0 GHz is the highest location accuracy of the keypad model at 100%. In addition, the RCS input parameters with both distances from the frequencies 3.0-5.0 GHz give the location accuracy of approximately 90% which is higher than the RCS input parameters with both distances from the frequencies 5.5-11.0 GHz of approximately

44.12%. And the power loss parameter with both distances in all frequencies give the location accuracy of approximately 31.31% which is less than the RCS input parameter with both distances in all frequencies.

Overall, the RCS input parameters have the location accuracy nearly twice the power parameters. The frequencies 3.0-5.0 GHz have considerably more the location accuracy than the frequencies 5.5-11.0 GHz. In addition, the distance of 29.50 cm has slightly more the location accuracy than the distance of 19.50 cm. These results show that the location accuracies get an effect from the parameters and the frequencies more than the distances so the parameters and the frequencies are going to be analyzed in the next sub-section, Discussion.

B. Discussion

As the results, the higher accuracy rate achieved with RCS is attributable to the RCS input parameters which are calculated from the object's scattering signals, while the power loss input parameters are determined from the signal loss. Thus, the RCS input parameters between different button-cells are more distinctive than the power loss parameters.

Figs. 8-10 illustrate the RCS input parameters in the frequencies 3.0-11.0 GHz at each Rx antenna; Rx1, Rx2 and Rx3, respectively and comparing between the RCS input parameters in the off-line phase and the RCS input parameters in the on-line phase of button-cell minus. Then, Figs. 11-13 show the power loss parameters in the frequencies 3.0-11.0 GHz at each Rx antenna; Rx1, Rx2 and Rx3, respectively and comparing between the power loss parameters in the off-line phase and the power loss parameters in the on-line phase of button-cell minus.

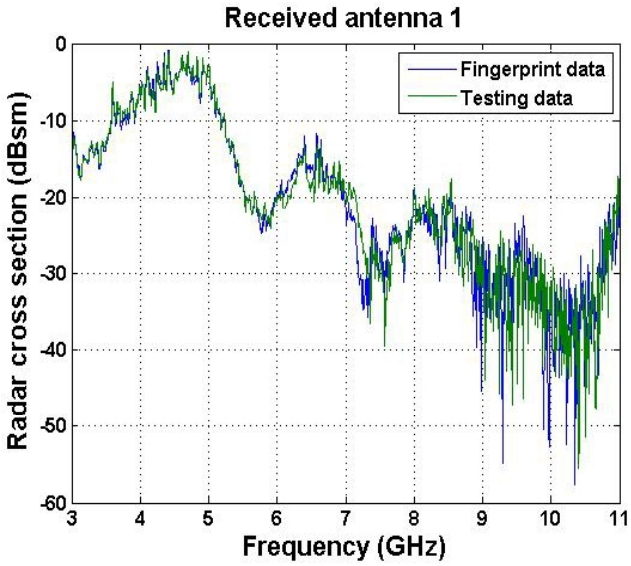

Fig. 8 the RCS at various frequencies with horizontal polarization (Rx1 location, button-cell minus)

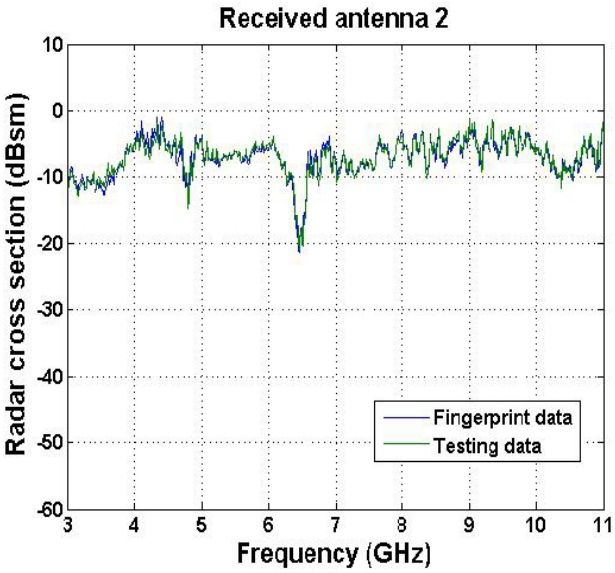

Fig. 9 the RCS at various frequencies with horizontal polarization (Rx2 location, button-cell minus)

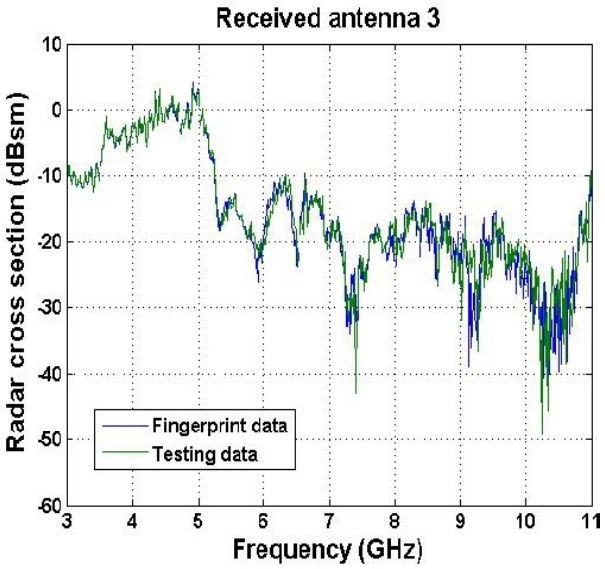

Fig. 10 the RCS at various frequencies with horizontal polarization (Rx3 location, button-cell minus).

Overall, it can be seen that the frequencies 3.0-5.0 GHz are less disturbed from noises than the frequencies 5.5-11.0 GHz so the variation between the RCS input parameters of the frequencies 3.0-5.0 GHz in the off-line phase and the RCS input parameters in the on-line phase is considerably less the RCS input parameters value than the frequencies 5.5-11.0 GHz. Moreover, the variation between the power loss parameters of the frequencies 3.0-5.0 GHz in the off-line phase and the RCS input parameters in the on-line phase is considerably less the power loss parameter value than the frequencies 5.5-11.0 GHz too. Similar results are obtained with other button-cells and Rx locations.

The RCS input parameters between different button-cells are more distinctive than the power loss parameters and the frequencies 3.0-5.0 GHz are more of the location accuracy for keypad model than the frequencies 5.5-11.0 GHz. Both distance results show that the hand could be detected in nearly accuracy although the hand would be changed level.

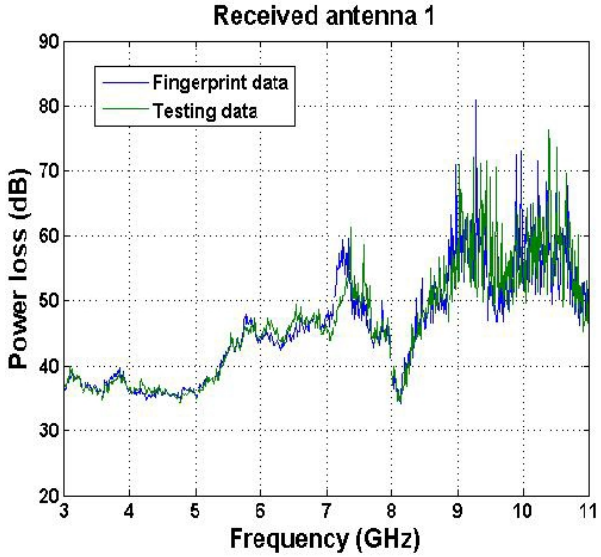

Fig. 11 The power loss at various frequencies with horizontal polarization (Rx1 location, button-cell minus)

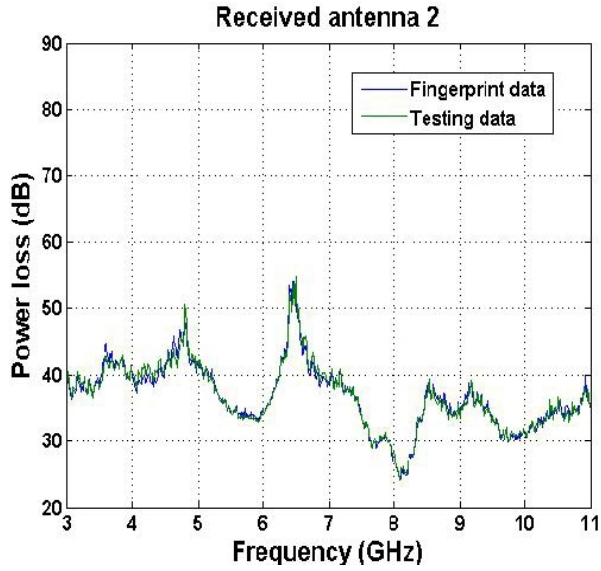

Fig. 12 The power loss at various frequencies with horizontal polarization (Rx2 location, button-cell minus)

V. Conclusion

In this paper, a 17-cell touchless keypad model is created in order to test for the tag-less for indoor localization of hand. The fingerprint-based indoor localization technique with minimum RMS error matching algorithm is used for the hand detection. The keypad model testing is conducted with 3 possible combinations (2x2x17) of three sets of criteria. The three sets of criteria are the parameters (i.e. the RCS parameters and the power loss parameter), distances (19.50 and 29.50 cm) and each frequency (3.0-11.0 GHz, varying 0.5 GHz).

The RCS input parameters have the location accuracy nearly twice the power parameter. Then, the frequencies 3.0-5.0 GHz have considerably more the location accuracy than the frequencies 5.5-11.0 GHz. Next, the distance of 29.50 cm has slightly more the location accuracy than the distance of 19.50 cm. Then, the highest location accuracy is a combination of the RCS parameters, 29.50 cm distance and 3.0 GHz.

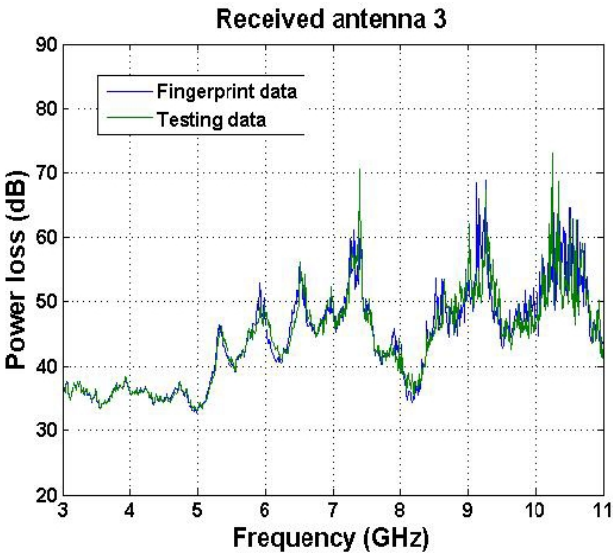

Fig. 13 The power loss at various frequencies with horizontal polarization (Rx3 location, button-cell minus).

For future work, we plan to use other methods of indoor localization working together with the RCS input parameters. Then, reflection and diffraction signal could be tested for the tag-less human localization. Next, an artificial intelligent might be used in order to increase an accuracy. After that, the human localization without tag will be tested in an indoor environment which is large areas.

Acknowledgment

The authors would like to express deep gratitude to King Mongkut's Institute of Technology Ladkrabang (KMITL) for a scholarship. In addition, sincere appreciation is extended to the participating volunteers for their contributions in the experiments.

References

[1] C. Nerguizian, C. Despins and S. Affès, "Geolocation in Mines with an Impulse Response Fingerprinting Technique and Neural Networks," Journal of Communications, Vol. 5, No. 3, pp. 603-611, March 2006.

[2] A. Toak, N. Kandil, S. Affès and S. Georges, "Neural Networks for Fingerprinting-Based Indoor Localization Using Ultra-Wideband," Journal of Communications. 01/2009.

[3] L. Zwirello, M. Janson, C. Ascher and U. Schwesinger, "Localization in Industrial Halls via Ultra-Wideband Signals," 2010 Workshop on Positioning Navigation and Communication, pp. 144–149, Mar. 2010.
[4] M. Stella, M. Russo and D. Begusic, "Location Determination in indoor Environment based on RSS Fingerprinting and Artificial Neural Network," Telecommunications, 2007, ConTel 2007, 9th International Conference on 13-15 June 2007, pp. 301-306.
[5] M. Zhou, Y. Xu and L. Tang, "Multilayer ANN indoor location system with area division in WLAN environment," Systems Engineering and Electronics, Journal of, vol. 21, no. 5, pp. 914–926, October 2010.
[6] M.L. Rodrigues, "Fingerprinting-Based Radio Localization in indoor Environment Using Multiple Wireless Technologies" 2011 IEEE 22nd International Symposium on Personal, Indoor and Mobile Radio Communications, pp 1203 - 1207.
[7] Z. Sahinoglu, S. Gezici and I. Guvenc, "Ultra-wideband Positioning Systems," New York: Cambridge University, Inc. 2008.
[8] C. Wu, Z. Yang, Y. Liu, and W. Xi, "WILL: Wireless Indoor Localization without Site Survey," IEEE Transactions on Parallel and Distributed Systems, Vol. 24, No. 4, April 2013.
[9] H. Liu, H. Darabi, P. Banerjee and J. Liu, "Survey of wireless indoor positioning techniques and systems," IEEE Transactions on Systems, Man, and Cybernetics Part C, vol. 37, no. 6, pp. 1067–1080, Nov. 2007.
[10] G. Mao and B. Fidan, "Localization Algorithms and Strategies for Wireless Sensor Networks," New York: Hershey, United States of America, 2009, ch. 3-5, ch. 11.
[11] A. Srikaew. "Computational Intelligence Book," https://sites.google.com/site/Computationalintelligencebook/download.
[12] L.C.D. Jong, and H.A.J. Herben, "A Tree-Scattering Model for Improved Propagation Prediction in Urban Microcells," IEEE Transactions on Vehicular Technology, vol. 53, no. 2, pp. 503-513, 2004.
[13] C. Lim, J.L. Volakis, K. Sertel, R.W. Kindt and A. Anastasopoulo, "Indoor Propagation models based on rigorous methods for site-specific multipath environment," IEEE Transactions on Antennas and Propagation, vol. 54, no. 6, pp. 1718-1725, 2006.
[14] M. Cheffena, "Physical-Statistical Channel Model for Signal Effect by Moving Human Bodies," EURASIP Journal on Wireless Communications and Networking, 2012:77, pp. 1-13, 2012.
[15] Understanding the FCC Regulations for Low-power, Nonlicensed Transmitters. Office of Engineering and Technology Federal Communications Commission, 1993.
[16] E.F. Knott, J.F. Shaeffer, and M.T. Tuley, "Radar Cross Section," Artech House, New Jersey. United States of America, 1985, ch. 1-2, ch. 5-6 and ch. 11.
[17] C. Ozdemir, "Inverse Synthetic Aperture Radar Imaging with MATLAB Algorithms," John Wiley & Sons, Inc., Hoboken, New Jersey. Singapore, 2012, ch. 2.
[18] B.R. Mahafza, "Radar Systems Analysis and Design Using MATLAB," Taylor & Francis Group, LLC, Chapman & Hall/CRC, 2nd ed. United States of America on acid-free paper, 2005, ch. 1.
[19] T.S. Rappaport, "Wireless Communications Principles and Practice," Prentice Hall PTR, 2nd ed. United States of America, 2002, ch. 4.
[20] S. Promwong, W. Hanitachi, J. Takada, P. Supanakoon and P. Tangtisanon, "Measurement and Analysis of UWB-IR Antenna Performance for WPANs," Thammasat International Journal of Science and Technology (TIJSAT), pp. 56-62, Oct-Dec 2003.
[21] S. Promwong, W. Hanitachi, J. Takada, P. Supanakoon and P. Tangtisanon, "Measurement and Analysis of UWB-IR Antenna Performance for WPANs," Thammasat International Journal of Science and Technology (TIJSAT), pp. 56-62, Oct-Dec 2003.